Biomedical Research **29** (6) 289-296, 2008

Topographic study on nerve-associated lymphatic vessels in the murine craniofacial region by immunohistochemistry and electron microscopy

Masahide FURUKAWA[1], Hiroshi SHIMODA[2], Tooru KAJIWARA[2], Seiji KATO[2] and Shigetaka YANAGISAWA[1]
[1] Department of Oncological Science and [2] Department of Anatomy, Biology and Medicine, Faculty of Medicine, Oita University, 1-1 Idaigaoka, Hasama-machi, Yufu-shi, Oita 879-5593, Japan

(Received 8 September 2008; and accepted 1 October 2008)

ABSTRACT

The distribution and fine structure of lymphatic vessels associated with nerves was studied by immunohistochemistry in the murine craniofacial region. The tissue sections and blocks were immunostained for LYVE-1, protein gene product 9.5, CD34 and aquaporin-1 to demonstrate the lymphatic vessels, nerves, blood vessels and water channel protein, respectively. Transmission electron microscopic examination was also performed to investigate the relationship between the lymphatics and nerves. In the nasal area, the lymphatics were found in dura mater on the cribriform plate and beneath the nasal mucosa, this supposedly supplying the cerebrospinal fluid drainage route along the olfactory nerves. The proximal portions of the cranial nerves were equipped with the lymphatics in the epineurium. In the distal portions of the nerves, the lymphatics were distributed in close proximity of the perineural sheath, and thus might contribute to maintenance of microenvironment suitable for the nerves by an absorptive activity of the lymphatic endothelial cells. The present findings suggest that the lymphatic system associated with the cranial nerves provides the pathway for transport of cerebrospinal fluid, tissue fluid, and free cells involved in immune response and tumor metastasis in the craniofacial region.

The lymphatic system plays a critical role in the transport of tissue fluid and immune cells, and as a route of tumor metastasis in the head and neck region. Several reports have described the lymphatic vessels associated with optic and olfactory nerves in the viscerocranial region of some mammals. The studies using injections of a silastic material such as Mirofil® (MV-122; Flow Tech Inc., Carver, MA) and/or dyes into the subarachnoidal space have demonstrated the nasal lymphatic vessels, and this implies the cerebrospinal fluid drainage route along the olfactory nerves into the nasal lymphatics (9, 12, 25, 27). Additionally in the optic nerve, the lymphatic vessels have been shown in the dura mater of the nerve sheath and thought to serve as drainage pathway of cerebrospinal fluid (5, 6, 11, 14). However, the distribution and structure of the lymphatic vessels in the cranial portion including the mandibular and maxillofacial region has not been fully clarified.

Meanwhile, in aspect of clinical medicine, sentinel lymph node navigation surgery, being contrived from the viewpoint of lymphatic metastasis route, has been recently established as an operative cure for malignant tumors in the head and neck region (1, 17). However, a number of cases involving skip and/or distant tumor metastases not via the sentinel lymph node in the head and neck cancer have been reported (3, 13, 26), and the metastatic pathway has not been analyzed. Thus, the precise organization of the lymphatic vessels in the craniofacial region should be defined for understanding functional significance of the lymphatic system and metastases of

Address correspondence to: Masahide Furukawa, M. D.
Department of Oncological Science, Faculty of Medicine, Oita University, 1-1 Idaigaoka, Hasama-machi, Yufu-shi, Oita 879-5593, Japan
Tel: +81-97-586-6703, Fax: +81-97-549-2838
E-mail: mfuruka@med.oita-u.ac.jp

malignant tumors.

Recent studies have provided novel molecules being specific to the lymphatic endothelial cells (2, 10, 15, 16), and an application of the molecular markers is useful for identifying the lymphatics in a variety of organs (22). The present study, therefore, demonstrates the lymphatic vessels associated with the cranial nerves as topography of lymphatic system in the murine craniofacial region by immunohistochemistry for the lymphatic hyaluronan receptor LYVE-1, being one of the recently identified lymphatic endothelium-specific markers.

MATERIALS AND METHODS

Animals. Adult BALB/cN Sea mice of both genders weighing 30–50 g were used in this study. They were kept under standard laboratory animal chow and water *ad libitum* under routine laboratory conditions. All experiments were adhered to the Guidelines for Animal experimentation of Oita University.

Tissue preparation. After the mice were sacrificed under deep anesthesia with an injection of sodium pentobarbital (50 mg/kg), the craniofacial regions were collected and placed in 4% paraformaldehyde in 0.1 M phosphate buffer (pH 7.4) for 20 h at 4°C. For transmission electron microscopic examination, some animals were perfused through cardiac left ventricle with physiological saline under deep anesthesia, followed by Karnovsky's fixative, and then the crania were dissected and immersed in the same fixative for longer than one day at 4°C.

Immunohistochemistry. The tissues fixed in a 4% paraformaldehyde solution were rinsed in the phosphate buffer and decalcified in 10% ethylene diamine tetra-acetic acid (EDTA; pH 7.4) for 2 weeks at 4°C. The decalcified specimens were dehydrated in graded ethanol series, embedded in paraffin, and cut into 5 μm thick sections. The deparaffinized sections were incubated in a 0.01 M citrate buffer (pH 6.0) at 121°C for 15 min to retrieve antigenicity of the objective proteins before immunostaining.

Immunostaining was performed as previously described (21, 23). Some tissue sections for light microscopy were immersed in 0.3% H_2O_2 in 1/15 M phosphate buffered saline (PBS; pH 7.4) containing 0.1% sodium azide (Wako Pure Chemical Industries, Osaka) at room temperature for 20 min to block the endogenous peroxidase activity. They were then treated with rabbit antibody against LYVE-1 (10 μg/mL; AngioBio, Del Mar, CA, USA), and subsequently with peroxidase (PO) or alkaline phosphatase (AP)-conjugated goat anti-rabbit IgG (Histofine Simple Stain; Nichirei Bioscience, Tokyo). The immunoreaction was detected by the diaminobenzidine (DAB; Dojindo, Kumamoto) or AP (Vector blue or red substrate kit; Vector Laboratories, CA, USA). For double immunostaining for LYVE-1 and CD34 or protein gene product (PGP) 9.5, some LYVE-1-immunostained sections were immersed in the citrate buffer at 95–99°C for 10 min to remove the precipitated antibodies from the tissues. They were then incubated in rat antibody to CD34 (diluted 1: 10; Abcam, Cambridge, UK) or PGP 9.5 (diluted 1: 3000; Ultraclone, Cambridge, UK), followed by the AP or PO-conjugated streptoavidin-biotin method (Vectastain ABC-AP or PO kit; Vector Laboratories). The site of immunoreaction was visualized by AP or DAB reaction. The immunostained sections were examined with a BX-60 light microscope (Olympus, Tokyo).

For fluorescence microscopy, some tissue sections were treated with a mixture of goat antibody to LYVE-1 (10 μg/mL; R&D Systems, Minneapolis, MN, USA), together with rabbit antibody to PGP 9.5 or aquaporin-1 (5 μg/mL; Chemicon International, Temecula, CA, USA), and then with a mixture of fluorescein isothiocyanate (FITC)-conjugated donkey anti-goat IgG (Jackson ImmunoResearch, West Grove, PA, USA) and indocarbocyanine (Cy3)-conjugated donkey anti-rabbit IgG (Jackson ImmunoResearch). The immunostained sections were examined by confocal laser scanning microscope (LSM5 PASCAL; Carl Zeiss, Oberkoehen, Germany).

Some residual tissue blocks were incubated in the antibody for LYVE-1, followed by AP-conjugated streptoavidin-biotin method, and the immunoreaction was detected by lead-based AP staining (20). The immunostained tissues were processed for scanning electron microscopy (SEM), and observed under a S-800 scanning electron microscope (Hitachi, Tokyo), as previously described (19).

Transmission electron microscopy (TEM). The crania fixed with Karnovsky's fixative was decalcified with 10% EDTA solution and then cut into small tissue pieces. The tissues were processed according to the method described in our previous reports (19, 22), and examined under a 1200EX transmission electron microscope (JEOL, Tokyo, Japan).

RESULTS

Immunohistochemistry for LYVE-1 exclusively dem-

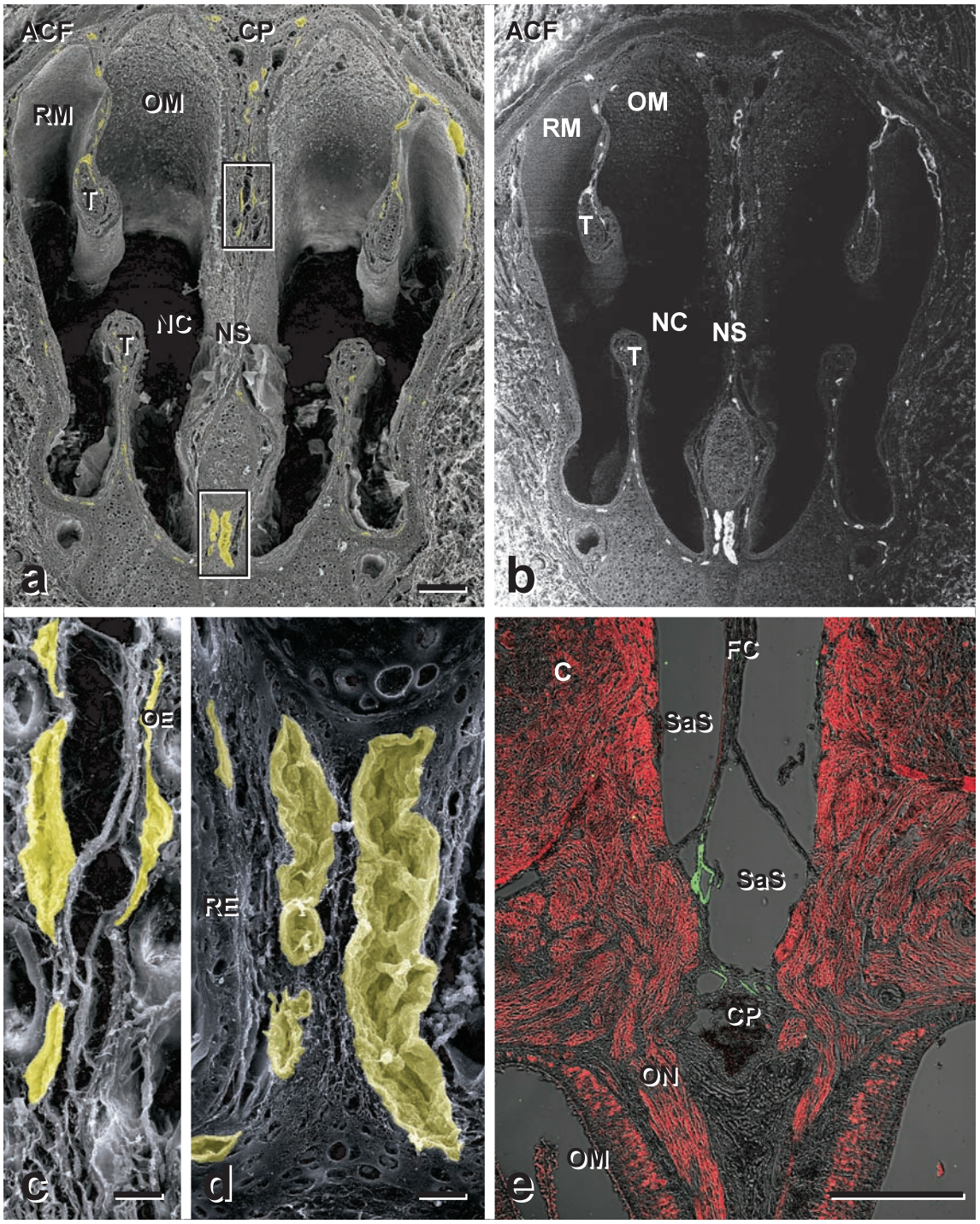

Fig. 1 SEM views of a frontal section (a-d) and fluorescence micrograph of a tissue section (e) from the murine cranio-nasal region immunostained for LYVE-1. **a:** Secondary emission image. The LYVE-1-immunopositive lymphatics colored yellow are seen beneath the cribriform plate (CP), nasal septum (NS), turbinates (T) and lateral walls of the nasal cavity (NC). ACF, anterior cranial fossa; OM, olfactory mucosa; RM, respiratory mucosa. **b:** Backscatter image of (a). The lymphatic endothelial cells are highlighted due to their LYVE-1 immunoreaction. **c, d:** Higher magnification of upper (c) and lower (d) boxed areas in **a**. The lymphatics (yellow) are close to the olfactory (OE) and respiratory (RE) epithelia. **e:** Nomarski differential interference-contrast images merged with fluorescence images. Double immunostaining for LYVE-1 (green) and PGP 9.5 (red). The LYVE-1-immunopositive lymphatics are shown in the dura mater on cribriform plate (CP) and Crista gali. The cerebrum (C), olfactory nerves (ON) and mucosae (OM) are immunostained for PGP 9.5. FC, Falx cerebri; SaS, subarachnoidal space. Scale bars 150 µm (a, b), 20 µm (c, d), 100 µm (e).

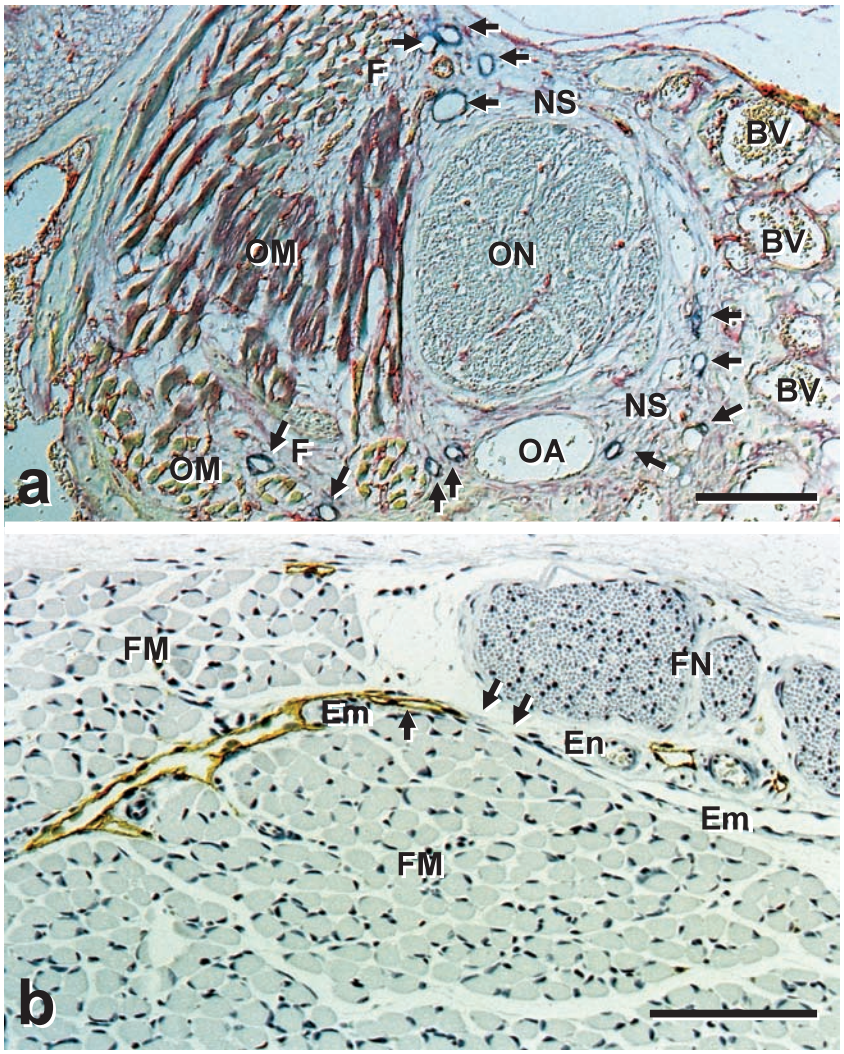

Fig. 2 Light micrographs of double immunostaining (a) for LYVE-1 (blue) and CD34 (red) and immunostaining (b) for LYVE-1 (brown) on tissue sections from the murine craniofacial region. **a:** The LYVE-1-immunopositive lymphatics (arrows) are seen in the neural sheath (NS) of the optic nerve and the fascia (F) of the ocular muscles. The blood vessels (BV) are immunostained for CD34. OA, ophthalmic artery. **b:** The LYVE-1-immunopositive lymphatics are seen in the epineurium (En) of the facial nerve (FN) and epimysium (Em) of the facial muscles (FM). The epimysium is continuous with the epineurium (arrows). Scale bars 200 μm (a), 100 μm (b).

onstrated lymphatic vessels with significant immunoreactivity in all preparations as reported in our previous studies (21–23). SEM examination of the LYVE-1-immunostained tissues further allowed a precise analysis of distribution and structure of the lymphatics. Since the lymphatic endothelial cells were highlighted by backscattered electron imaging (BEI) due to the immunoreaction, the lymphatics could be easily identified even in secondary electron imaging (SEI) by contrasting the BEI with the SEI. On the other hand, immunostaining for PGP 9.5 and CD34 defined neuronal components and small blood vessels, respectively.

Lymphatics in the nasal region

In the nasal region, the nasal mucosa beneath the cribriform plate, nasal septum and lateral walls including turbinates were richly supplied with the lymphatic vessels (Fig. 1a–d). The lymphatic capillaries, consisting only of attenuated endothelial cells, were disposed beneath the epithelium of both the olfactory mucosa (Fig. 1c) and the respiratory mucosa (Fig. 1d). The olfactory nerves themselves were not endowed with the lymphatics, but the dura mater on the cribriform plate and Crista gali involved the lymphatic capillaries in the internal cranial base of mice (Fig. 1e).

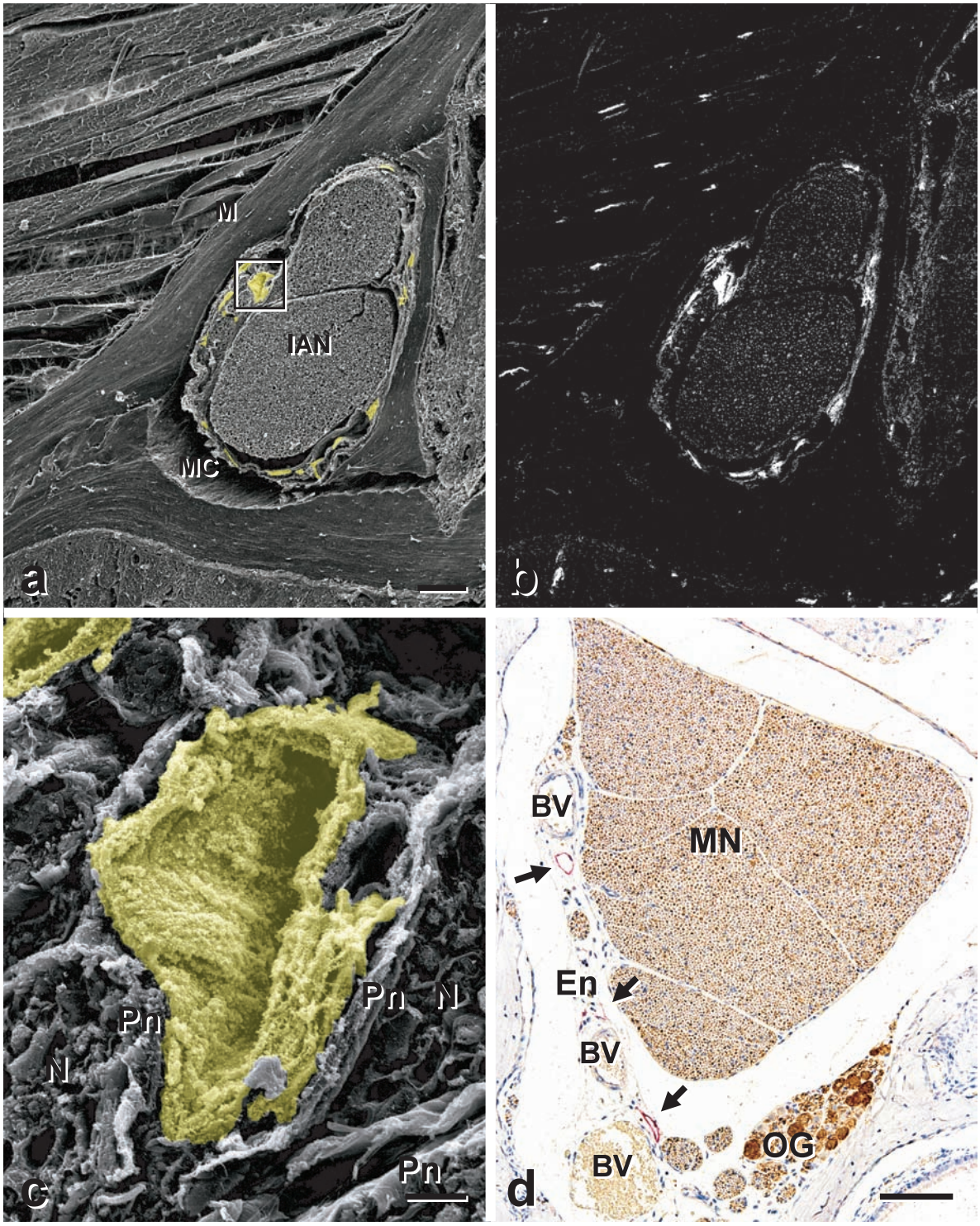

Fig. 3 SEM views of a frontal section and a light micrograph of a tissue section from the murine mandibular region immunostained for LYVE-1. **a:** Secondary emission image. The LYVE-1-immunopositive lymphatics colored yellow are seen in the neural sheath of the inferior alveolar nerve (IAN) running through the mandibular canal (MC). M, mandible. **b:** Backscatter image of **a**. The lymphatic endothelial cells are highlighted due to their LYVE-1 immunoreaction. **c:** Higher magnification of the boxed area in **a**. The lymphatics (yellow) are close to the perineurium (Pn) of the nerves (N). **d:** Double immunostaining for LYVE-1 (red) and PGP 9.5 (brown). In the proximal portion of the mandibular nerve (MN), the LYVE-1-immunopositive lymphatics (arrows) are seen only in the epineurium (En). BV, blood vessels; OG, otic ganglion. Scale bars 55 µm (a, b), 5 µm (c), 100 µm (d).

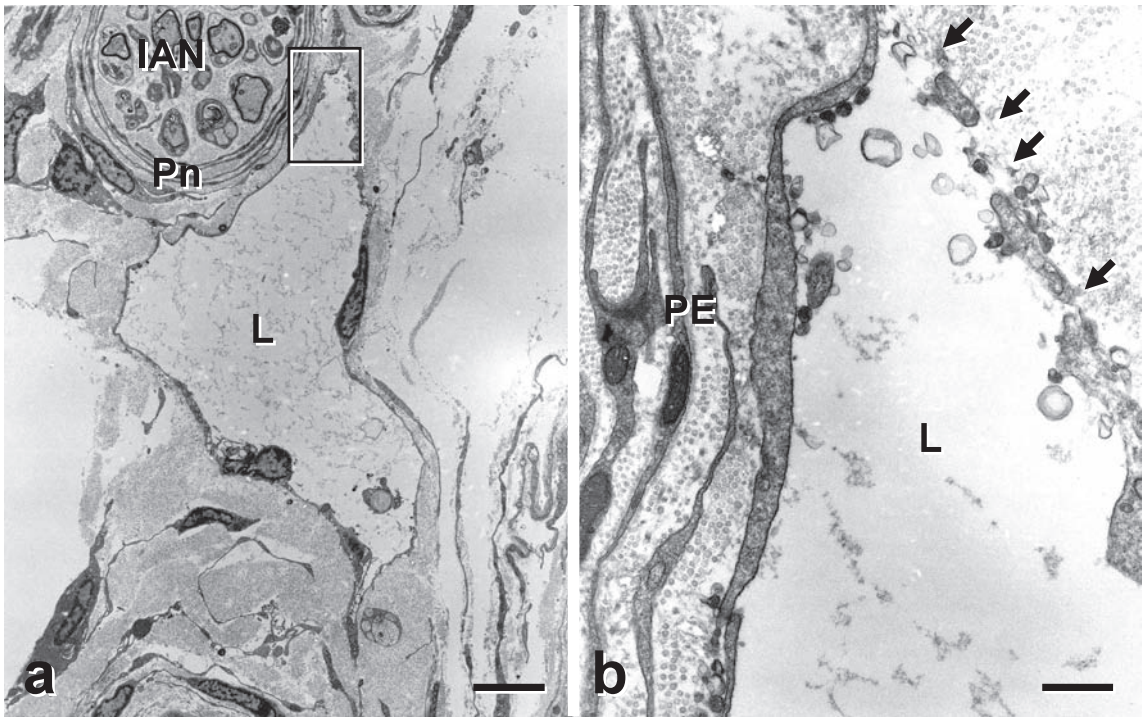

Fig. 4 TEM views of the murine mandibular canal. **a:** A lymphatic vessel (L) is seen just beneath the perineurium (Pn) of the inferior alveolar nerve (IAN). **b:** Higher magnification of the boxed area in **a**. The lymphatic endothelial cells are in close proximity to the perineural epithelium (PE). Arrows indicate gaps between the endothelial cells. L, lymphatic. Scale bars 5 μm (a), 500 nm (b).

Lymphatics in the orbit and facial muscular region
In the orbit, the lymphatic vessels were abundantly distributed in the dural sheath of the optic nerve and the fascia (epimysium) of the ocular muscles (Fig. 2a). The facial nerves and muscles also exhibited the lymphatics in the epineurium and the epimysium, respectively (Fig. 2b). The epineural sheaths were often continuous with the epimysium of the neighboring muscles, and many lymphatics were arranged in the connective tissue layers (Fig. 2).

Lymphatics in the maxillary and mandibular region
The proximal portions of the maxillary and mandibular nerves predominantly showed the lymphatic vessels in their epineurium, but neither in the perineurium and endoneurium (Fig. 3d). The superior and inferior alveolar nerves, which ran through the mandibular canal as branches of the maxillary and mandibular nerves, were equipped with many lymphatics in the epineurium even within the bone (Fig. 3a, b). The superior alveolar nerves also revealed a similar organization of the lymphatics to that related to the inferior alveolar nerves as mentioned above. SEM examination further demonstrated that some of the lymphatic capillaries were in close proximity to the perineurium of the nerves (Fig. 3c). Under TEM, the lymphatic capillaries, being composed only of attenuated endothelial cells, were often in close location to perineural epithelium, leaving a narrow space measuring 50–300 nm (Fig. 4). The lymphatics, being concomitant with the alveolar nerves, further displayed many gaps between the endothelial cells in some parts at the opposite side of the perineurium consisting of multilayered perineural cells (Fig. 4b). In our SEM examination has not so far shown cytoplasmic fenestration in the endothelial cells of the perineural lymphatic vessels.

To inspect the ability of water transfer of the nerve-associated lymphatics, double immunostaining for aquaporin-1 and LYVE-1 was performed. Aquaporin-1 was principally immunolocalized in the LYVE-1-immunopositive lymphatics in the neural sheaths (Fig. 5).

DISCUSSION

The present study is first to delineate the structural organization of the lymphatic vessels associated with the cranial nerves by immunohistochemical

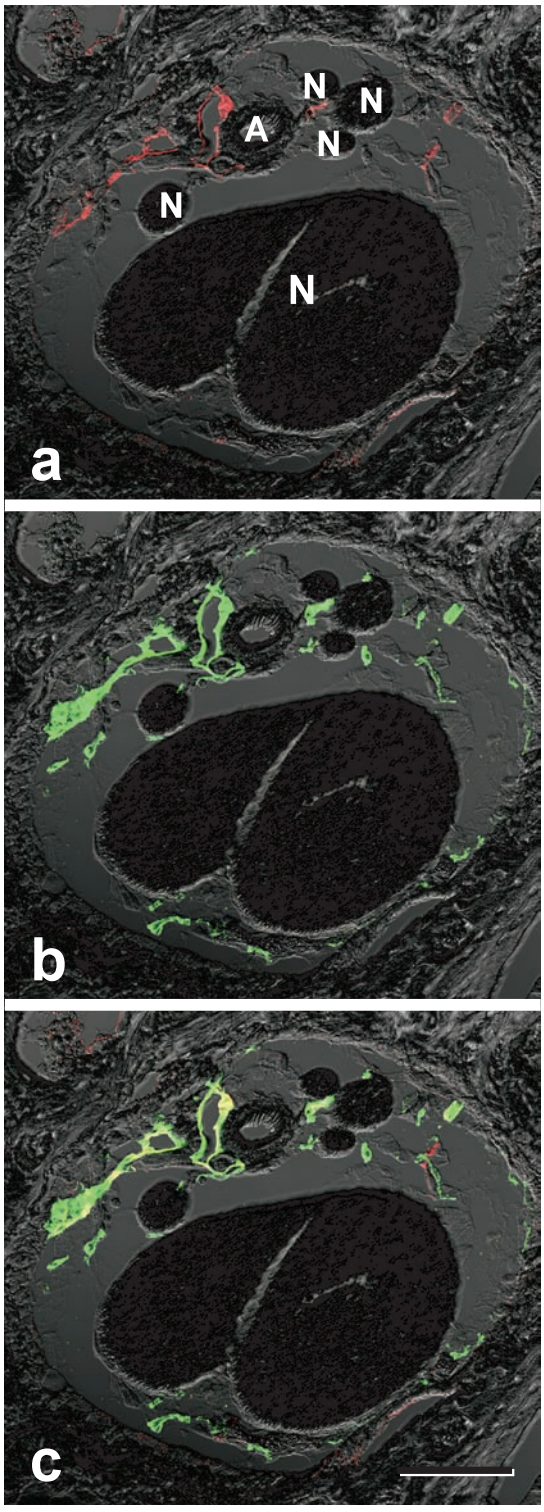

Fig. 5 Fluorescence micrographs of double immunostaining for aquaporin-1 (a, red) and LYVE-1 (b, green) on a tissue section of the murine mandibular canal. Figure **c** shows a merged image. The immunoreaction products for aquaporin-1 are predominantly localized in the LYVE-1-immunopositive lymphatics (yellow in c) distributed in the sheaths of the nerves (N). A, arteriole. Scale bar 100 μm.

method. Application of immunohistochemistry for LYVE-1 to such specimens as tissue sections and blocks is useful for demonstrating the cranial lymphatic system in the murine cranium.

The present histochemical findings in the nasal region indicate a possible drainage route for cerebrospinal fluid along the olfactory nerves in the mouse, as reported in the other mammals including sheep (9), pig (12), lamb (27) and rat (12, 25). Our immunohistochemical examination further disclosed the lymphatic vessels in the dura mater on the cribriform plate within the murine neurocranium, thus implying that the cerebrospinal fluid drainage from the subarachnoidal space to the nasal lymphatics might—at least partly—commence with the intracranial dural lymphatics. Meanwhile, a recent research indicated that the perineurium in itself was extension of arachnoid, drainage road of cerebrospinal fluid, and it was assumed that this was equal with "Keiraku" in Oriental medicine (8). It seems that more studies are necessary about cerebrospinal fluid circulation.

The murine optic nerves were equipped with the lymphatics in their epineurium, as previously described in the other mammals (5, 6, 11, 14), and the ocular muscles disposed the lymphatics in the epimysium continuous with the epineural sheath. Since the proximal portions of the other cranial nerves except for the olfactory one and the surrounding muscles also displayed a similar distribution of the lymphatics, it appeared to be characteristic of the lymphatic vessels in the cranial area to run in the connective tissue layer ranging between epineurium and epimysium.

The peripheral portions of the cranial nerves, in contrast, exhibited the lymphatic capillaries closely associated with the perineurium; interestingly, the alveolar nerves were, even within the bone, supplied with the lymphatics by their perineural sheath. The perineurium comprises blood-nerve barrier by tight junctions of the multilayered perineural cells (18, 24), but such low weight molecules as ions and glucose are known to transfer across the barrier via specific transporters and channels (4, 7). The existence of many gaps between the lymphatic endothelial cells and of aquaporin-1, which is a representative water channel protein, on the endothelial cell membrane of the lymphatic vessels adjacent to the perineurium, indicates a high absorptive potential of the lymphatics. These findings imply that the lymphatics drain the tissue fluid involving water and some molecules, and free cells to coordinate microenvironment outside the barrier for proper neuro-

transmission. However, in this study, the gaps were seen in only the other side of perineurium. A further study seems to be needed about accurate distribution of the gaps.

In conclusion, the present results suggest that the lymphatic vascular system associated with the cranial nerves contributes not only milieu beneficial to neuronal activity, but also the pathway to transport of cerebrospinal fluid, tissue fluid and free cells in the craniofacial region. Furthermore, the present data on the cranial lymphatic pathway provide a morphological basis for routes of immune cell transfer and tumor metastasis, although further studies are needed to understand the pathological role of the lymphatic system.

REFERENCES

1. Alvarez Amézaga J, Barbier Herrero L, Pijoan del Barrio JI, Martín Rodríguez JC, Romo Simón L, Genolla Subirats J, Rios Altolaguirre G, de los Ríos A, Arteagoitia Calvo I, Landa Llona S, Arruti González JA, López Cedrún J and Santamaría Zuazua J (2007) Diagnostic efficacy of sentinel node biopsy in oral squamous cell carcinoma. Cohort study and meta-analysis. *Med Oral Pathol Oral Cir Bucal* **12**, E235–243.
2. Breitender-Geleff S, Matsui K, Soleiman A, Meraner P, Poczewski H, Kalt R, Schaffner G and Kerjaschki D (1997) Podoplanin, novel 43-kd membrane protein of glomerular epithelial cells, is down-regulated in puromycin nephrosis. *Am J Pathol* **151**, 1141–1152.
3. Byers RM, Weber RS, Andrews T, McGill D, Kare R and Wolf P (1997) Frequency and therapeutic implications of "skip metastases" in the neck from squamous carcinoma of the oral tongue. *Head Neck* **19**, 14–19.
4. Froehner SC, Davies A, Baldwin SA and Lienhard GE (1988) The blood-nerve barrier is rich in glucose transporter. *J Neurocytol* **17**, 173–178.
5. Gausas RE, Gonnering RS, Lemke BN, Dortzbach RK and Sherman DD (1999) Identification of human orbital lymphatics. *Opthal Plast Reconstr Surg* **15**, 252–259.
6. Gausas RE, Daly T and Fogt F (2007) D2–40 expression demonstrates lymphatic vessel characteristics in the dural portion of the optic nerve sheath. *Ophtal Plast Reconstr Surg* **23**, 32–36.
7. Handberg A, Kayser L, Høyer PE and Vinten J (1992) A substantial part of GLUT-1 in crude membranes from muscle originates from perineuronal sheaths. *Am J Physiol* **262**, 721–727.
8. Hashimoto PH (2002) The lympholiquid system vs. cardiovascular system. A new concept of the double circulatory system of the body. In: *Proceedings of the 7th World Congress for Microcirculation*, pp. 375–379.
9. Johnston M, Armstrong D and Koh L (2007) Possible role of the cavernous sinus vein in cerebrospinal fluid absorption. *Cerebrospinal Fluid Res* **4**, 3. (Open Access)
10. Joukov V, Pajusola K, Kaipainen A, Chilov D, Lahtinen I, Kukk E, Saksela O, Kalkkinen N and Alitalo K (1996) A novel vascular endothelial growth factor, VEGF-C, is a ligand for the Flt4 (VEGFR-3) and KDR (VEGFR-2) receptor tyrosine kinases. *EMBO J* **15**, 290–298.
11. Killer HE, Laeng HR and Groscurth P (1999) Lymphatic capillaries in the meninges of the human optic nerve. *J Neuro-Ophtalmol* **19**, 222–228.
12. Koh L, Zakharov A, Nagra G, Armstrong D, Friendship R and Johnston M (2006) Development of cerebrospinal fluid absorption sites in the pig and rat: connections between subarachnoid space and lymphatic vessels in the olfactory turbinates. *Anat Embryol* **211**, 335–344.
13. Kowalski LP, Bagietto R, Lara JR, Santos RL, Tagawa EK and Santos IR (1999) Factors influencing contralateral lymph node metastasis from oral carcinoma. *Head Neck* **21**, 104–110.
14. Ludemann W, Berens von Rautenfeld D, Samii M and Brinker T (2005) Ultrastructure of the cerebrospinal fluid outflow along the optic nerve into the lymphatic system. *Childs Nerv Syst* **21**, 96–103.
15. Petrova TV, Mäkinen T, Mäkelä TP, Saarela J, Virtanen I, Ferrell RE, Finegold DN, Kerjaschki D, Yla-Hertteala S and Alitalo K (2002) Lymphatic endothelial reprogramming of vascular endothelial cells by the Prox-1 homeobox transcription factor. *EMBO J* **21**, 4593–4599.
16. Prevo R, Banerji S, Ferguson DJ, Clasper S and Jackson DG (2001) Mouse LYVE-1 is an endocytic receptor for hyaluronan in lymphatic endothelium. *J Biol Chem* **276**, 9420–9430.
17. Ross GL, Soutar DS, Gordon MacDonald D, Shoaib T, Camilleri I, Roberton AG, Sorensen JA, Thomsen J, Grupe P, Alvarez J, Barbier L, Santamaria J, Poli T, Massarelli O, Sesenna E, Kovács AF, Grünwald F, Barzan L, Sulfaro S and Alberti F (2004) Sentinel lymph node biopsy in head and neck cancer: Preliminary results of a multiple trial. *Ann Surg Oncol* **11**, 690–696.
18. Shanthaveerappa TR and Bourne GH (1962) The 'perineural epithelium', a metabolically active, continuous, protoplasmic cell barrier surrounding peripheral nerve fasciculi. *J Anat (Lond)* **96**, 527–537.
19. Shimoda H (1998) Structural organization of lymphatics in the monkey esophagus as revealed by enzyme-histochemistry. *Arch Histol Cytol* **61**, 439–450.
20. Shimoda H, Kudo T, Takahashi Y and Kato S (2000) Ultrastructural and histochemical characterization of special muscle cells in the monkey small intestine. *Arch Histol Cytol* **63**, 217–228.
21. Shimoda H, Takahashi Y and Kato S (2004) Regrowth of lymphatic vessels following transection of the muscle coat in the rat small intestine. *Cell Tissue Res* **316**, 325–338.
22. Shimoda H and Kato S (2006) A model for lymphatic regeneration in tissue repair of the intestinal muscle coat. *Int Rev Cytol* **250**, 73–108.
23. Shimoda H, Bernas MJ, Witte MH, Gale NW, Yancopoulos GD and Kato S (2007) Abnormal recruitment of periendothelial cells to lymphatic capillaries in digestive organs of angiopoietin-2-deficient mice. *Cell Tissue Res* **328**, 329–337.
24. Thomas PK (1963) The connective tissue of peripheral nerve: an electron microscopic study. *J Anat (Lond)* **97**, 35–44.
25. Walter BA, Valera VA, Takahashi S and Ushiki T (2006) The olfactory route for cerebrospinal fluid drainage into the peripheral lymphatic system. *Neuropathol Appl Neurobiol* **32**, 388–396.
26. Woolger JA (1999) Pathology of the N0 neck. *Br J Oral Maxillofac Surg* **37**, 205–209.
27. Zakharov A, Papaiconomou C and Johnston M (2004) Lymphatic vessels gain access to cerebrospinal fluid through unique association with olfactory nerves. *Lymphat Res Biol* **2**, 139–146.